Journal of Molecular Structure 1202 (2020) 127350

Contents lists available at ScienceDirect

Journal of Molecular Structure

journal homepage: http://www.elsevier.com/locate/molstruc

X-ray crystallography and molecular dynamics studies of the inclusion complexes of geraniol in β-cyclodextrin, heptakis (2,6-di-O-methyl)-β-cyclodextrin and heptakis (2,3,6-tri-O-methyl)-β-cyclodextrin

Elias Christoforides, Katerina Fourtaka, Athena Andreou, Kostas Bethanis*

Physics Laboratory, Department of Biotechnology, Agricultural University of Athens, 75 Iera Odos, 11855, Athens, Greece

ARTICLE INFO

Article history:
Received 10 October 2019
Received in revised form
1 November 2019
Accepted 1 November 2019
Available online 5 November 2019

This paper is dedicated to the memory of Prof. Dimitris Mentzafos.

Keywords:
Geraniol
β-Cyclodextrin
Heptakis(2,6-di-O-methyl)-β-cyclodextrin
Heptakis(2,3,6-tri-O-methyl)-β-cyclodextrin
Crystal structure
Molecular dynamics

ABSTRACT

The inclusion of the linear monoterpene, geraniol (*gr*) in β-cyclodextrin (β-CD), heptakis(2,6-di-O-methyl)-β-cyclodextrin (DM-β-CD) and heptakis(2,3,6-tri-O-methyl)-β-cyclodextrin (TM-β-CD) has been studied by X-ray crystallography and Molecular Dynamics simulations. The *gr*/β-CD complex crystallizes as a head-to-head dimer in the $P2_1$ space group stacking along the crystallographic *a*-axis in a channel packing mode. Two guest molecules are accommodated almost axially inside the dimeric cavity with their aliphatic ends laying in the interface region of the dimer facing each other and their hydroxylic ends protruding from the narrow β-CD rims. The guest molecules of the adjacent dimers in a channel are interconnected via CH ···O and hydrogen bonds forming an internal wire. Both the *gr*/DM-β-CD and *gr*/TM-β-CD complexes crystallize in the $P2_12_12_1$ space group and stack along the crystallographic *b*-axis in a head-to-tail manner. DM-β-CD host adopts the conformation of a rigid and well-shaped open cone upon complexation, in which the guest molecule is found highly disordered over 5 sites with varying depths of immersion. The *gr*/DM-β-CD complex units are arranged in channels and the *gr* molecules within these channels are also interconnected via CH ···O bonds. On the other hand, TM-β-CD host is found severely distorted adopting a 'closed' cup-shaped conformation. The guest is partially encapsulated in the wide rim of TM-β-CD and it is found disordered over 3 sites with quite different orientations. The complex units are arranged forming screw channels, with the main part of the guest laying outside the host cavity and filling the intermediate space between the succeeding hosts. The MD analysis based on the crystallographically determined structures sheds light on the dynamic behavior of the geraniol upon complexation with these hosts, its conformation variations and the interconversion of the inclusion modes in solution. Finally, MM/GBSA-calculations revealed that the ascending order in binding affinity ΔG values is: *gr*/TM-β-CD < *gr*/DM-β-CD < *gr*/β-CD.

1. Introduction

Geraniol (3,7-dimethyl-2,6-octadien-8-ol, *gr*) is an acyclic monoterpene alcohol (Fig. 1a) and a natural component of the essential oil of many plant species like citronella, palmarosa and notably roses [1]. Besides its use as fragrance chemical [2], geraniol exhibits a broad spectrum of biological activities as it can be considered as an antimicrobial [3,4], antioxidant [5], repellent against mosquitoes [6] and antitumor agent that can also prevent acute allograft rejection [7,8]. Although geraniol is considered to be a weak allergen [9], its use as bioinsecticide could mitigate the harmful effects of synthetic chemicals on pollination insects like bees [10]. Like other monoterpenes [11,12], geraniol is insoluble in water and extremely volatile, properties that make its use in perfumery, cosmetics, drug and food industries problematic [13]. To this end, the inclusion of geraniol in Cyclodextrins (CDs) has attracted increasing interest as it offers optimized physicochemical properties and is considered as promising bioactive material for designing functional food [14,15]. CDs having the shape of a truncated cone with hydrophilic outer surface and lipophilic cavity can form supramolecular complexes with a wide variety of hydrophobic guest molecules that are commonly used in food [16], agricultural [17] and pharmaceutical [18] industries. Despite its low water solubility, β-cyclodextrin (Fig. 1b) is widely used for the formation

* Corresponding author.
E-mail address: kbeth@aua.gr (K. Bethanis).

https://doi.org/10.1016/j.molstruc.2019.127350
0022-2860/

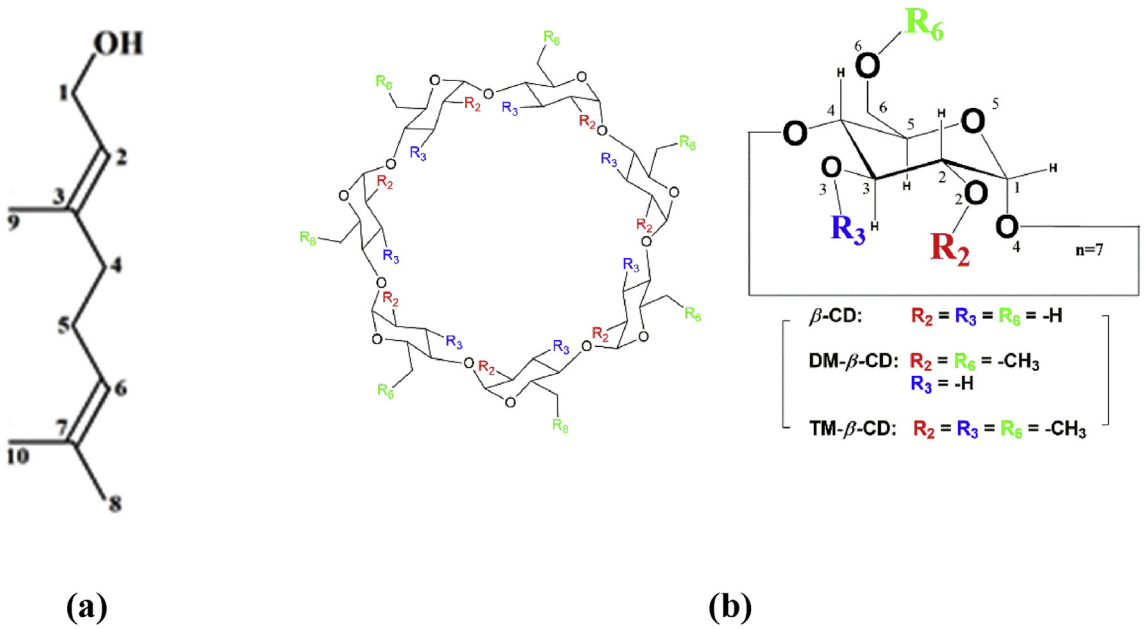

Fig. 1. Schematic representation of: **(a)** geraniol and **(b)** β-cyclodextrin, heptakis (2,6-di-O-methyl)-β-cyclodextrin and heptakis (2,3,6-tri-O-methyl)-β-cyclodextrin.

of such inclusion compounds due to its suitable cavity size, its high availability and low cost. The methylated derivatives of β-CD: 2,6-di-*O*-methyl-β-Cyclodextrin and 2,3,6-tri-*O*-methyl-β-Cyclodextrin (DM-β-CD and TM-β-CD, respectively, Fig. 1b) have also attracted interest as they exhibit an increased aqueous solubility and inclusion capacity compared to their parent β-CD [19].

Inclusion of geraniol in β-CD has been previously characterized by gas chromatography (GC), nuclear magnetic resonance (^{1}H NMR), differential scanning calorimetry (DSC), scanning electron microscopy (SEM), phase solubility studies and infra-red (IR) spectroscopy [14,20,21]. Moreover, a crystal structure of the inclusion complex crystallizing in the *P*1 space group, has been presented by Ceborska et al. [22].

In this study, we present the crystal structures of the inclusion complexes of geraniol with i) β-CD, where the inclusion complex is found crystallized in a different form (space group $P2_1$ and complex units arranged according to a Channel packing mode) than that previously reported by Ceborska et al. [22], revealing a polymorphism for this inclusion complex, ii) DM-β-CD and iii) TM-β-CD. Moreover, based on the atomic coordinates determined by the X-ray crystallography, molecular dynamics (MD) simulations for the three inclusion compounds in explicit water solvent were performed with the aim to monitor the dynamic behavior of geraniol in different hosts, study the different inclusion modes and calculate the host-guest binding affinity in each case. The findings provide a detailed picture of the inclusion of geraniol in native and methylated β-CDs enlightening the role of the stability of the host cavity in the inclusion complex formation.

In a past paper [23], we had presented the crystal structures and MD simulations for the inclusion complexes of β-citronellol in the same host molecules (β-CD, DM-β-CD and TM-β-CD). β-citronellol is also a natural acyclic monoterpenoid alcohol, whose chemical structure is similar to that of geraniol, having a double bond less and hence an extra torsional degree of freedom. In this work, we compare the inclusion complexes of geraniol and β-citronellol in the same hosts (binding modes, guest and host conformation, dynamic behavior in solution, binding affinity), in order to examine how the conformational freedom of the guest affects the inclusion mode in β-CD, DM-β-CD and particularly in TM-β-CD where the induce-fit mechanism is more pronounced. The information provided by these studies sheds light on the formation and stability of geraniol inclusion complexation with native and methylated β-CD and aids the creation of geraniol-CD systems with optimized physicochemical properties as new ecological and efficacious products [24,25].

2. Materials and methods

2.1. Sample preparation and crystallization

Geraniol as a colorless, not miscible in water liquid (98% pure, d = 0.884 g/mL) was purchased from Alfa Aesar (part of Thermo Fisher Scientific Co LLC) whereas cyclodextrins (β-CD, DM-β-CD and TM-β-CD) as white powders (>90% pure) from Cyclolab (Budapest, Hungary). All reagents were used as received.

Crystals of the inclusion compound of *gr*/β-CD were formed by using the slow cooling crystallization technique. Briefly, 14 μL of geraniol were added in a 5 mL equimolar aqueous solution of β-CD (0.08 mmol, ~0.016 M), stirred at 70 °C for 1 h and the final mixture was gradually cooled to room temperature over a period of one week. In the cases of methylated CDs, crystals were formed by adding suitable amounts of geraniol in a 0.3 M aqueous solution of DM-β-CD or a 0.05 M aqueous solution of TM-β-CD in a host:guest molar ratio of 1:1, respectively. The final mixtures were stirred at room temperature for 30 min and then were maintained in a water bath at 48 °C for a period of two weeks.

2.2. X-ray crystallography

In the cases of *gr*/β-CD and *gr*/TM-β-CD inclusion complexes, data were collected using synchrotron radiation light ($\lambda = 0.81$ Å) at the EMBL Hamburg (X11 beamline) at the DORIS stage ring, DESY. Single crystals were picked with cryo-loops and flash cooled under the N_2 stream to 100 K using paraffin oil as cryoprotectant. The diffracted x-ray intensities were recorded on a marCCD 165 detector and they were initially processed by using the XDS program [26]. A semi-empirical absorption correction using SADABS [27] was applied after integration and conversion of the output HKL file

with the utility program *xds2sad* [28]. The crystal structures were determined by the molecular replacement method (program DIRDIF2008 [29]) using as initial models the atomic coordinates of the inclusion complexes of (-)-α-terpineol/β-CD [22] and indolebutyric acid/TM-β-CD [30] in the cases of *gr*/β-CD and *gr*/TM-β-CD respectively.

In the case of *gr*/DM-β-CD, data were measured at 100(2) K on a home-source Bruker D8-VENTURE diffractometer, using *CuKa* radiation (λ = 1.54 Å) and an Oxford Cryosystems low-temperature device. The APEX 3 software was used for data collection and data processing. Data integration and global-cell refinement was performed with the program *SAINT* [31]. Absorption correction was performed with *SADABS* [27]. The structure solved by Patterson-seeded dual-space recycling with the *SHELXD* program [32].

In all cases, the structures were refined by full-matrix least squares against F^2 using the *SHELXL-2014/7* program [33] through the WINGX suite [34] and the *SHELXLE GUI* [35]. Due to the limited resolution and structural complexity of the model, soft restraints on bond lengths and angles of the guest molecule were applied using the *PRODRG2* webserver [36]. In order to maintain a high data/parameters ratio, anisotropic thermal parameters were imposed to selected, non-H atoms of the host molecules. All H-atoms of the host molecules were placed geometrically for temperature of 100 K and allowed to ride on the parent atoms. *U*iso(H) values were assigned in the range 1.2−1.5 times *U*eq of the parent atom.

Structural analysis and figures preparation were performed with the graphics programs Mercury, PyMOL and Olex2 [37−39] for all three crystal structures. Crystallographic information files with embedded structure factors have been deposited into the Cambridge Structural Database (CSD) under the deposition numbers CCDC: 1955632, 1955635 and 1955636. Table 1 also lists some parameters relative to the crystal data and structure refinement of the three complexes.

2.3. Molecular dynamics

Molecular dynamics simulations of all three inclusion complexes in explicit aqueous solution have been conducted using the Amber12 software package [40] and the CLYCAM [41] for native β-CD and AMBER-compatible q4md-CD force fields [42] for DM-β-CD and TM-β-CD atoms, respectively. The starting atomic coordinates were taken from the determined crystal structures of *gr*/β-CD, *gr*/DM-β-CD and *gr*/TM-β-CD inclusion complexes. GAFF parameters and AM1BCC charges were applied to the guest molecule using ANTECHAMBER [43].

A water octahedral shell of 10 Å thickness was added to solvate the systems with the TIP3P water model. MD calculations and minimizations were carried out with the program SANDER. Periodic boundary conditions were imposed by means of the particle mesh Ewald method using a 10 Å limit for the direct space sum. The detailed simulation protocol for 12 ns has been analytically described in a previous work [44]. Root mean square deviation (RMSD) calculations and geometric analysis were performed by CPPTRAJ [45] and VMD [46].

Moreover, the binding free energy $\Delta G_{(GB)}$ between the bound and unbound state of the solvated host and guest molecules energy for each complex was computed also by the well-known MM/GBSA (Molecular Mechanics-Generalized Born Surface Area) method

Table 1
Crystal data and structure refinement statistics.

	geraniol/β-CD	geraniol/DM-β-CD	geraniol/TM-β-CD
Crystal data			
Chemical formula	$2(C_{42}H_{70}O_{35})\cdot 2(C_{10}H_{18}O)\cdot 16(H_2O)$	$C_{56}H_{98}O_{35}\cdot C_{10}H_{18}O\cdot 10(H_2O)$	$C_{63}H_{112}O_{35}\cdot C_{10}H_{18}O\cdot 0.5(H_2O)$
M_r	1417.22	1637.58	1591.76
Crystal system, space group	Monoclinic, $P2_1$	Orthorhombic, $P2_12_12_1$	Orthorhombic, $P2_12_12_1$
Temperature (K)	100	100	100
a, *b*, *c* (Å)	15.580 (5), 24.980 (2), 18.680 (2)	18.247 (1), 19.264 (1), 24.171 (2)	14.903 (6), 20.888 (1), 27.686 (8)
β (°)	110.91 (2)	–	–
V (Å^3)	6791 (3)	8496.8 (9)	8618 (4)
Z	4	4	4
Radiation type	Synchrotron, λ = 0.8148 Å	Cu *Ka*, λ = 1.5418 Å	Synchrotron, λ = 0.8160 Å
μ (mm^{-1})	0.17	0.93	0.13
Crystal size (mm)	0.2 × 0.2 × 0.1	0.2 × 0.2 × 0.1	0.3 × 0.2 × 0.1
Data collection			
Diffractometer	Synchrotron	Bruker *APEX*-II	Synchrotron
Absorption correction	Multi-scan	Multi-scan SADABS2016/2 - Bruker AXS area	Multi-scan
T_{min}, T_{max}	*SADABS* 2014/5 0.509, 0.778	detector scaling and absorption correction 0.545, 0.752	*SADABS* 2014/5 0.684, 0.746
No. of measured, independent and observed [$I > 2s(I)$] reflections	31126, 14314, 12191	65446, 12233, 8816	87735, 11978, 10712
R_{int}	0.064	0.080	0.06
θ_{max} (°)	25.2	59.1	26.7
$(\sin\theta/\lambda)_{max}$ (Å^{-1})	0.523	0.556	0.550
Refinement			
$R[F^2 > 2s(F^2)]$, $wR(F^2)$, *S*	0.084, 0.258, 1.12	0.088, 0.252, 1.02	0.071, 0.187, 1.06
No. of parameters	1243	1163	1100
No. of restraints	108	307	148
H-atom treatment	H-atoms treated by a mixture of independent and constrained refinement	H-atoms treated by a mixture of independent and constrained refinement	H atoms treated by a mixture of independent and constrained refinement
$\Delta\rho_{max}$, $\Delta\rho_{min}$ (e Å^{-3})	0.63, −0.51	0.55, −0.45	0.57, −0.45
Absolute structure parameter	0.0 (2)	0.04 (9)	−0.14 (14)

[47]. The entropic term $T\cdot\Delta S$ was also calculated from normal mode analysis using the respective module of Amber and thus the estimation of the absolute binding free energy $\Delta G_{(all)}$ value was carried out according to:

$$\Delta G_{(all)} = \Delta G_{(GB)} - T\Delta S$$

However, the estimation of the entropic term by the normal analysis is often problematic as it lacks information of the conformational entropy. Alternative methods do not give converged results [48]. Thus, the comparison of the binding affinities between the examined inclusion complexes is based on the $\Delta G_{(GB)}$ term solely.

3. Results and discussion

3.1. The gr/β-CD complex

3.1.1. Description of the structure

The *gr*/β-CD inclusion complex crystallized in the $P2_1$ space group with lattice parameters quoted in Table 1. Its asymmetric unit contains two β-CD molecules (denoted as host A and host B), two *gr* molecules and 16 water molecules distributed over 29 sites. Host A and host B form, the commonly observed in β-CD inclusion complexes, head-to-head type dimer stabilized via intermolecular hydrogen bonds between their O3*n*-H ($n = 1, \ldots 7$) hydroxyl groups and intramolecular hydrogen bonds between the O2*n*-H and the O3(*n*+1)-H hydroxyls of adjacent glucopyranose units in each host molecule.

The guest/host stoichiometry of the inclusion complex is 2:2 as each β-CD molecule hosts in its hydrophobic cavity one geraniol molecule. Each guest molecule is found disordered over two sites as follows: the guest in the host A cavity occupies the sites *gr*1A (site occupation factor, s.o.f.: 60%) and *gr*2A (s.o.f.: 40%) whereas the guest in the host B cavity occupies the sites *gr*1B (s.o.f.: 60%) and *gr*2B (s.o.f.: 40%). The geometry and the occupancy factors of the occupied sites, indicate that the encapsulated guests can co-exist only as *gr*1A-*gr*1B or *gr*2A-*gr*2B pairs (Fig. 2a). The dimeric complexes are arranged forming channels along the *a*-axis (a detailed description of the crystal packing is given in paragraph 3.1.2). In every case, the guest molecules are accommodated almost axially inside the dimeric cavity with their terpene backbones (mean axis along C1−C2−C3−C4−C5−C6−C7 atoms, see Figs. 1a and 2a) forming angles with the approximate seven-fold β-CD molecular axis in the range of 4.2°−27.1°. The aliphatic ends of the guests, lay in the interface region of the dimer, facing each other and forming closed shell interactions between each other and with the inner H3 atoms of the β-CD hydrophobic cavities. Closed shell interactions are also observed between the C9 methyl groups of the guests occupying *gr*1A-*gr*1B sites and the inner H5 atoms of the β-CD. The hydroxylic ends of the guests protrude from the narrow β-CD rims, participating in various directional interactions with the guest and host molecules of the adjacent dimeric complex of the channel (Supplementary Table S1). According to these interactions, the protruding part of the *gr*1A site can form hydrogen and CH ···O bonds with the guest in the host B of the adjacent dimer when this guest occupies the sites *gr*2B and *gr*1B respectively. On the other hand, a dimer which contains guests at sites *gr*2A-*gr*2B is sterically hindered to be preceded or followed by a dimer which contains guests at the same sites. Therefore, the channel is formed by dimers with guests that their position alternates mainly from the pair *gr*1A - *gr*1B to *gr*2A-*gr*2B. This alternation is interrupted by dimers containing guests at positions *gr*1A - *gr*1B (never at *gr*2A-*gr*2B), thus justifying the occupancy of 60% and 40% for the *gr*1A - *gr*1B and *gr*2A-*gr*2B pairs respectively (Fig. 2b, Table S1).

3.1.2. Conformation of the β-CD molecules and crystal packing

In the Supplementary Table S3a, some geometric parameters defining the conformation of the two β-CD molecules are listed. The glucosidic O4*n* atoms of both host molecules form nearly regular heptagons as indicated by their distances from their approximate centroids and their deviations from the O4*n* mean plane. Small and positive tilt angles (τ) are observed between the optimum O4n plane and the mean plane of the O4(n-1) ….C1n … C4n … O4n atoms of each glucose unit (ranging from 3.4087(12) to 13.696(5)° for host A and 1.9617(7) to 11.907(4)° for host B) indicating that the primary sides of the host β-CDs incline towards the approximate sevenfold axis of the cavity. The orientations of the O6−H groups are dependent on the direction of hydrogen bonding with nearby acceptors and donors (guest, water and CD molecules). Almost all the primary hydroxyl groups of both hosts A and B have the *gauche-gauche (gg)* conformation pointing outwards the cavity, hydrogen bonded with bridging water molecules. Only one primary hydroxyl of host A (O65A which is hydrogen bonded with the guest of the subsequent dimer in the channel and/or with O65B) and a disordered primary hydroxyl of host B (O65B hydrogen bonded with O65A above) have the *gauche-trans* (gt) conformation pointing inwards the cavity.

The β-CD dimers stack along the *a*-axis, the angle between their approximate seven-fold axis and *a*-axis being 10.63°. The water molecules are distributed in the intermolecular voids acting as hydrogen bonding mediators to stabilize the entire crystal (Fig. 2c and Supplementary Table S2a). The packing mode of the dimeric structure is characterized as Channel (*CH*) as the shift between two successive dimers along the *a*-axis (2.87 Å) is very close to the average value of 2.7 Å observed in such cases ($P2_1$ space group) according to the classification by Metzafos et al. [49] (Fig. 2b and c). A thorough search in the Cambridge Structural Database (CSD) [50] based on unit cell dimensions similarity resulted in 26 entries, 10 of which bear upon CD inclusion complexes that crystallize in $P2_1$ space group. Among them, the (−)-α-terpineol and (+)-α-terpineol complexes in β-CD are described as narrow channels (*CH*) running along the *a* crystallographic axis [22] with the displacement between two successive dimers along the *a*-axis being equal to 2.88 Å.

On the other hand, in the case of the crystal structure of *gr*/β-CD crystallized in *P*1, previously reported by Ceborska et al. [22], this value is equal to 6 Å, implying an Intermediate (*IM*) packing mode along *c* axis (Fig. 3). In that structure, the geraniol molecules are encapsulated in the β-CD dimer similar to our structure. However, they adopt a more extended conformation (the distance between the O1 and C7 atom of each guest is 8.095(3) and 8.404(3) Å) compared to our case (O1 to C7 distances vary from 7.042(4) to 7.686(3) Å). Therefore, the length of the encapsulated pair of guests is quite larger, the distance between the oxygen atoms O1A and O1B of the protruding hydroxyls of the guests in the dimer is 16.740(3) Å in the structure crystallized in *P*1 whereas it is 15.421(3) Å (pair *gr*1A-*gr*1B) and 14.455(2) Å (pair *gr*2A-*gr*2B) in our case. As a result, in the case of the structure crystallized in *P*1, the guests protrude significantly higher from the narrow rims of the dimer not allowing the formation of channels and their hydroxyls are hydrogen bonded with the hosts of adjacent dimers that are significantly shifted (Fig. 4). In our case, the dimeric complex units are aligned in channels which contain geraniol molecules interconnected via hydrogen bonds and thus forming a wire. The ability of the guest geraniol molecule to adopt more and less extended conformations is also examined with MD studies of the inclusion complexes in aqueous environment (see paragraph 3.4 below) by monitoring these geometric features in the time frame of the simulations.

Thus, *gr*/β-CD presents polymorphism: form I crystallized in *P*1 according to *IM* packing mode and form II crystallized in $P2_1$

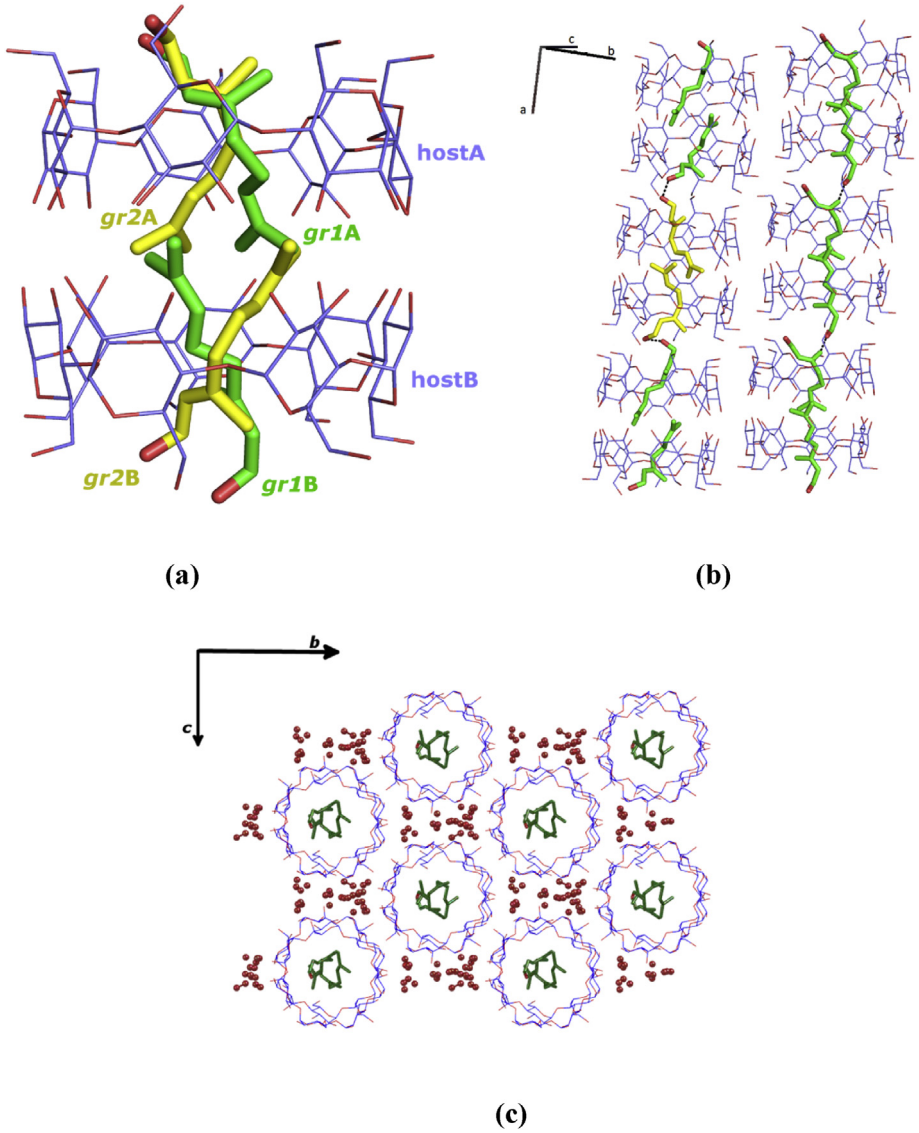

Fig. 2. The inclusion complex of *gr*/*β*-CD (Form II). **(a)** The host:guest stoichiometry is always 2:2. Guests coexist inside the dimeric cavity in pairs of *gr*1A and *gr*1B (green, s.o.f.: 60%) or *gr*2A and *gr*2B sites (yellow, s.o.f.: 40%) **(b)** the crystal packing is characterized as Channel (*CH*). Guests of adjacent dimers in the channel are interconnected forming a wire and **(c)** crystal packing projection along the *a*-axis. A network of water molecules (red) contributes in the crystal packing by bridging adjacent channels. Water molecules in (a) and (b) as well as hydrogen atoms in all figures are omitted for clarity.

according to *CH* packing mode. As the degree of hydration differs in the two above forms (form I has 10.5 and form II 16 water molecules in the asymmetric unit), one could characterize forms I and II as pseudopolymorphic. However, in both forms the columns of the inclined dimers (in the case of form I) or channels (in the case of form II), are not formed via water mediated interactions but rather via interactions between the guest and the host or the guest of the adjacent dimer. These interactions are correlated with the varying conformation of the guests.

By comparing the crystal structure of *gr*/*β*-CD with that of *β*-citronellol/*β*-CD previously reported by Fourtaka et al. [23], we observe that the guests in both inclusion complexes are encapsulated in *β*-CD dimers with the same stoichiometry and inclusion mode. However, the unit cell, the space group (*P*1) and the crystal packing (*IM*) of *β*-citronellol/*β*-CD crystal structure are similar to that of form I of *gr*/*β*-CD. The *β*-citronellol molecules, although they have an extra torsional degree of freedom compared to *gr* molecules, they also adopt an extended conformation in the *β*-CD dimeric cavity (O1 to C7 distance 8.200(3) and 8.198(3) Å; distance between the oxygen atoms O1A and O1B of the protruding hydroxyls of the guests in the dimer = 16.865(4) Å), protruding high enough from the narrow rims of the dimer to prohibit the formation of channels.

3.2. The gr/DM-β-CD complex

3.2.1. Description of the structure

The *gr*/DM-*β*-CD inclusion complex crystallizes in the $P2_12_12_1$ space group with lattice parameters quoted in Table 1. Its asymmetric unit consists of one DM-*β*-CD molecule hosting a highly disordered geraniol molecule (1:1 host:guest stoichiometry) and 10 waters distributed over 12 sites (Fig. 4a). The guest geraniol molecule does not interact with the host capsule by any specific directional interaction and it is found distributed over 5 occupied

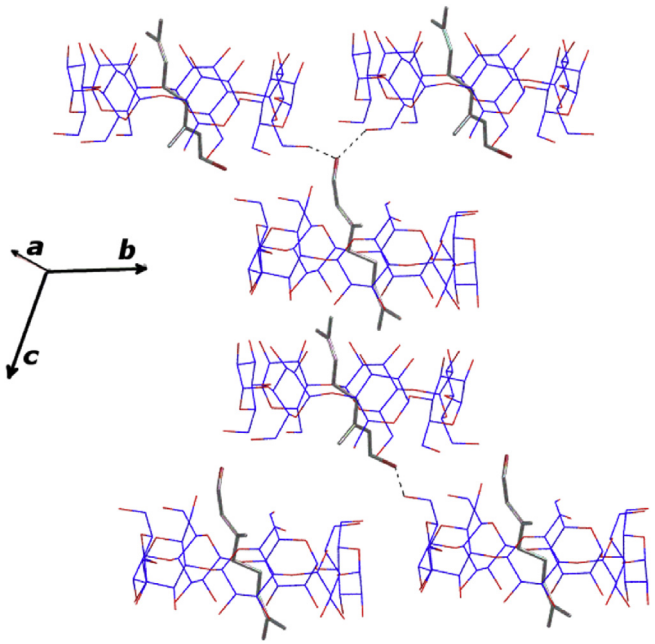

Fig. 3. Crystal packing of form I of *gr*/*β*-CD crystallizing in *P*1 [22]. The dimers are arranged according to the *IM* packing mode forming H-bonds between the hydroxyl of the guest geraniol and the primary hydroxyls of the *β*-CDs of the adjacent dimers. Hydrogen atoms and water molecules are omitted for clarity.

sites of 20% occupancy each. All sites are accommodated axially inside the hydrophobic DM-*β*-CD cavity having an extended conformation (distance between O1 and C7 varies from 7.404 to 8.113 Å) with their hydroxylic ends protruding from the primary rim of the host (distance between O1 of the occupied sites and O4 mean plane of the host varies from 5.816 Å to 8.011 Å), entering into the secondary rim of the adjacent host of the formed channel (Fig. 4a; a detailed description of the crystal packing is given in the following paragraph 3.2.2.). The guest occupying a particular site can coexist with the guest of the adjacent complex of the channel occupying the same or other sites (there are various sterically allowed combinations) connected to it with CH ···O bonds between the hydroxyl of the one guest and a methyl group (C9 or C10) of the aliphatic end of the other. Thus, as in the case of the *gr*/*β*-CD (Form II), a wire of interconnected geraniol molecules is also formed inside the channel (Fig. 4b).

3.2.2. *Conformation of the DM-β-CD molecule and crystal packing*

The host DM-β-CD molecules are exceptionally stabilized upon complexation with *gr* molecules. The geometric features reported in Table S3b, indicate that the host molecules retain their torus like macrocycle shape and the round conformation. This is due to the formation of the well-known intramolecular interglucose O3(n)—H···O2(n + 1) hydrogen bonds [51]. These intramolecular H-bonds are predominant in host DM-*β*-CD conformation as they stabilize the glucopyranose units forming a rigid host cavity. The inclusion complexation with the stiff linear guest *gr* molecule seems to aid further the hosting DM-*β*-CD to retain its well-formed truncated cone shape. A characteristic geometric feature showing this formation is the angle τ reported in the Supplementary Table S3b, (τ = tilt angle between the optimum O4n plane and the mean plane atoms O4(n − 1), C1n, C4n, O4n) indicating the inclination of the glucopyranose units towards the O4n plane. In the case of the *gr*/DM-β-CD complex, the range of the values of this angle is rather limited, namely 9.40(2)° - 17.35(4)°. The corresponding values for the *β*-citronellol/DM-*β*-CD complex [23] vary from 5.02° to 24.59°. The induce-fit mechanism is more pronounced in the case of the later complex as *β*-citronellol, with a torsional degree of freedom more than *gr*, has the flexibility to fit better in the rigid cavity of the host forming a more stable inclusion complex with DM-*β*-CD as it is shown in the paragraph 3.4 of the MD studies below.

On the other hand, in the case of the *gr*/DM-β-CD complex, the guest *gr*, being less flexible than *β*-citronellol, is found highly disordered, occupying five sites of different rotation about the sevenfold axis of the host macrocycle and different immersion depth in the cavity of the host. The high disorder of the guest *gr* is due mainly to the open truncated cone conformation of the host that allows the high protrusion of the guest from its narrow rim, the limited flexibility of the guest and the lack of any directional interactions between the guest and the host. The slight inclination of the guest occupying some of these sites, results to the observed alternation of the conformation of the primary methoxy groups of DM-*β*-CD. Among the 3 fully occupied primary methoxy sites, 2 of them are found to have the *gt* and one the *gg* conformation, while the 4 disordered methoxy groups adopt both conformations (Table S3b).

The hosts are arranged co-axially so that the wide rim (head) of the one faces the narrow rim (tail) of the other (head-to-tail mode) forming antiparallel columns along the *b* axis. The displacement of two successive complexes of the same column is 0.61 (5) Å and the angle between their O4n mean planes equals to 2.43(6)° indicating a channel packing mode. Additionally, the shifting of the adjacent channels is 16.457(2) Å and the angle between their O4n mean planes equals to 2.30(6)°. The guests, as mentioned above, are partially located in the intermediate space between two succeeding hosts of a channel, aiding the observed Channel packing mode (Fig. 4a and b). Furthermore, the adjacent channels are glued via hydrogen bonds with bridging water molecules. Supplementary Table S2b, summarizes the main hydrogen bonds that are observed between the hosts and the water molecule bridges.

A search in the CSD resulted in only one entry that shares similar cell dimensions and the same space group with the investigated structure. This inclusion complex (adamantanol/DM-*β*-CD, CCDC code: BEFJOL) forms monomers with host:guest stoichiometry of 1:1 and illustrates the same packing mode (antiparallel channels along b) with the *gr*/DM-*β*-CD complex. It is interesting that the inclusion complexes of the linear molecule of geraniol and that of the bicyclic molecule of adamantanol in DM-*β*-CD have the same crystal packing. In both cases, the complex units are rather rigid and the channel formation is not aided by adjacent host interactions but solely by the interactions between the guests of the adjacent complex units. In the case of the adamantanol/DM-*β*-CD, the adjacent bicyclic guests in the channel are linked via two bridging water molecules entrapped inside the hydrophobic host cavity. Moreover, the formed channels in both complexes (*gr* and adamantanol in DM-*β*-CD) are glued by exactly the same number of water molecules (10 in the asymmetric unit; there are 12 water molecules in the asymmetric unit of adamantanol/DM-*β*-CD but two of them are found inside the cavity). This explains the relative high hydration degree for DM-*β*-CD complexes that is observed in these two cases.

On the other hand, in the case of the inclusion complex of *β*-citronellol in DM-*β*-CD, the guest, which is similar to *gr*, although is oriented similarly in the DM-*β*-CD cavity, it has a less extended conformation than *gr* due to its extra torsional degree of freedom. In particular, the distance between its O1A and C7A atoms is 6.640(2) Å and 7.628(2) Å for the two occupied sites. Thus, *β*-citronellol does not protrude from the primary rim of the DM-*β*-CD (distance between O1 of the guest and O4 mean plane of the host being 3.685(4) Å and 4.827(3) Å for the two occupied sites) and no channels of complex units are formed. The crystal packing of *β*-

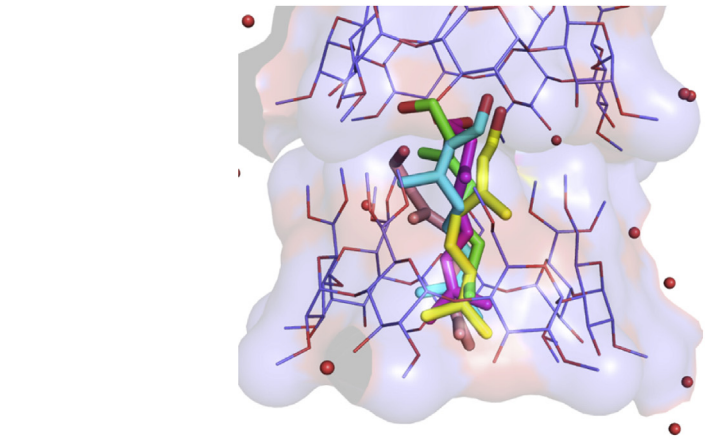

(a)

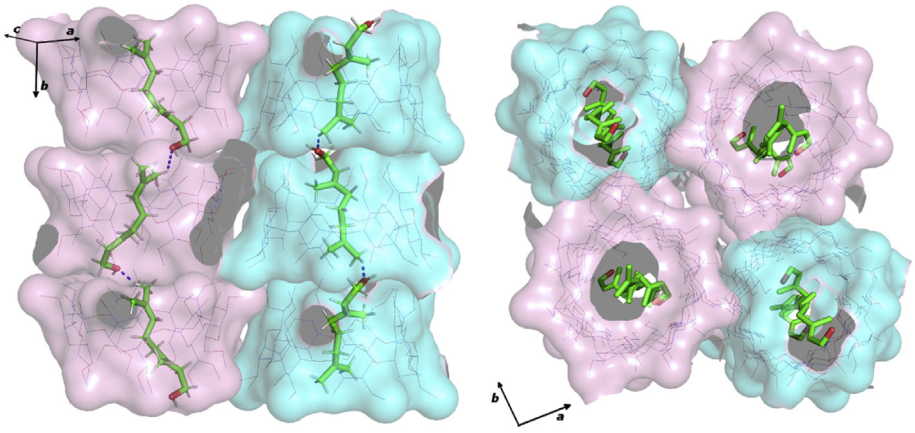

(b)

Fig. 4. (**a**) The inclusion compound of *gr*/DM-*β*-CD (host:guest ratio 1:1). The highly disordered guest protrudes from the narrow rim of the rigid host and enters into the wide rim of the adjacent host (**b**) the crystal packing consists of antiparallel channels along the *b* axis hosting interconnected guests that form a wire (left); projection of the crystal packing mode on the *ab* plane (right). Hydrogen atoms and water molecules are omitted for clarity.

citronellol/DM-*β*-CD complex is that of a herringbone and the hydration degree is 4.3 water molecules in the asymmetric unit as commonly observed in the DM-*β*-CD inclusion complexes.

3.3. The gr/TM-β-CD complex

3.3.1. Description of the structure

The *gr*/TM-*β*-CD inclusion complex crystallizes in the orthorhombic $P2_12_12_1$ space group. Unit cell parameters and further crystal lattice details are quoted in Table 1. The asymmetric unit consists of one TM-*β*-CD molecule, one geraniol molecule disordered over three sites *gr*1, *gr*2 and *gr*3 (s.o.f.: 60%, 20% and 20% respectively) and a water molecule site with occupation factor of 0.5.

The observed inclusion modes of the *gr* in TM-*β*-CD are affected by two main factors: the stiff extended conformation of the guest and the 'closed' cup-shaped conformation of the flexible host. In all three occupied sites, *gr* has an extended conformation (O1 to C7 distance varies from 7.537(2) to 8.384(3) Å) and is accommodated inclined with respect to the 7-fold molecular axis of the host with its main part protruding from the wide rim of the host. The host TM-*β*-CD is severely distorted due to the absence of the intramolecular interglucose hydrogen bonds in permethylated cyclodextrins, forming the characteristic 'lid' in its primary rim, commonly observed in the majority of the TM-*β*-CD complexes [51].

The guest occupying the *gr*1 site lies along the diameter of the oval shaped macrocycle of the host near its secondary rim. Its hydroxyl group forms a hydrogen bond with the methoxy O22 atom of the host's secondary methoxy group (Supplementary Table S2c), while its aliphatic tail protrudes from the secondary rim of the host and is mainly located in the interspace between adjacent inclusion complexes (Fig. 5a and b). The occupied site *gr*2 is also partially located in the wide rim of the host having the opposite orientation to that of *gr*1: its aliphatic end is located in the hydrophobic cavity (distance between C7 and mean plane of O4n atoms 0.84(4) Å) whereas its hydroxyl protrudes from the secondary rim of the host hydrogen bonded with the sole, half-occupied, water molecule site (Supplementary Table S2c). Finally, the occupied site *gr*3 has a more axial accommodation in the cavity of the host. Its hydroxyl points towards the narrow rim of the host, opposite to the hydroxyl of the site *gr*1, and it forms CH ···O bonds with the primary methoxy

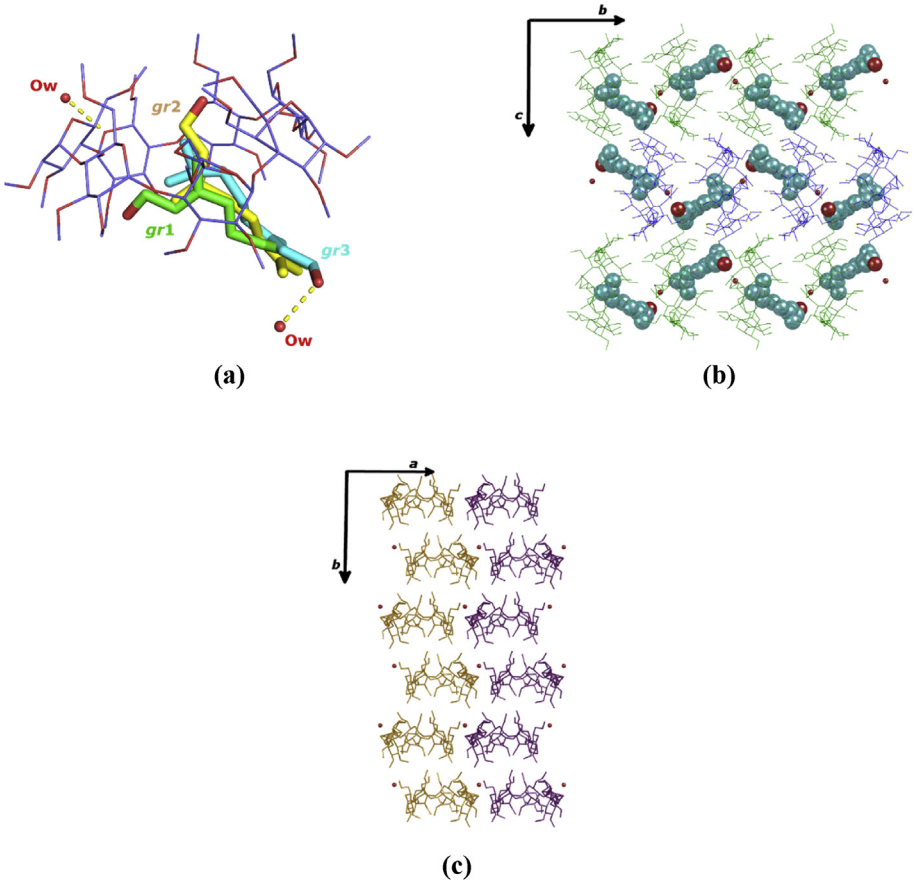

Fig. 5. **(a)** The inclusion compound of *gr*/TM-*β*-CD. The guest is disordered over three sites: *gr*1 (green with s.o.f. 60%), *gr*2 (yellow with s.o.f. 20%) and *gr*3 (cyan with s.o.f. 20%), **(b)** complex units in a head to tail mode form antiparallel screw channels along the *b* axis and **(c)** projection of crystal packing on the *ab* plane, guest molecules are omitted for clarity. Hydrogen atoms are omitted for clarity.

group of the 6th glucopyranose unit (G6) of the host (Supplementary Table S2c). This site has the most extended conformation of all three *gr* occupied sites and the main part of its aliphatic end protrudes from the wide rim of the host (Fig. 5a and b).

3.3.2. *Conformation of the TM-β-CD molecule and crystal packing*

Geometrical characteristics and parameters regarding the TM-*β*-CD conformation are given in Supplementary Table S3c. As it is mentioned above, TM-*β*-CD is found severely distorted due to the absence of the intramolecular interglucose hydrogen bonds that are observed in the cases of the *gr* inclusion complexes in *β*-CD and DM-*β*-CD hosts. The glucosidic O4n atoms deviate significantly from their mean plane (range: −0.556(3) Å to 0.609(3) Å) forming an elliptical heptagon. Additionally, the values of the distances between the O4n atoms and the centroid of their mean plane also vary (range: 4.66(4) Å to 5.22(4) Å) indicating a distorted macrocycle. The observed methylglucose ring tilt angle values span a wide range from −13.90(2)° to 43.3(2)° contributing to the narrowing of the primary and the broadening of the secondary rim. Five residues have positive tilt angles indicating that their primary sides incline towards the approximate sevenfold axis of the macrocycle whereas two methyl-glucose residues (G2 and G6) have negative tilt angles inclining outwards the host cavity. G1, G5 and G7 form the characteristic 'lid' in the primary region of the host that is usually observed in TM-*β*-CD inclusion complexes, preventing the deep penetration of the guest. The O5*n*-C5*n*-C6*n*-O6*n* torsion angles indicate that the primary methoxy groups (two of them are found disordered) have the usual gauche-gauche (*gg*) and *gauche*-trans (*gt*) conformation.

The complex units are arranged in a head-to-tail mode along the *b*-axis forming screw-channels (Fig. 5b and c). In each column, the shift between alternate host molecules is 3.30(2) Å and the angle between their O4n mean planes is 11.33(3)°. Parallel and antiparallel columns are arranged along *a*- and *c*-axis respectively, stabilized by a large number of intermolecular C—H ...O bonds between the adjacent hosts. The sole water molecule that partially (50%) occupies the site OW1 is hydrogen bonded with the etheric O54 atom of the host and the hydroxyl of the guest occupying the site *gr*3 (20%) (Supplementary Table S2c). This crystal packing mode characterizes several isostructural TM-*β*-CD complexes not only with other linear guests like *β*-citronellol (DEWMIE) [23], but also with more bulky molecules like pesticide fenitrothion (CIJVEY) [52] and the cyclic 3-cyclooctyl-1,1-dimethylurea (OYAPIO) [53].

In particular, in the case of the inclusion complex of *β*-citronellol in TM-*β*-CD, the inclusion mode of the guest is similar to that of the *gr*1 occupied site (60%) of *gr*/TM-*β*-CD. The main difference is that the guest *β*-citronellol, having a torsional degree of freedom more than *gr*, adopts a more bent conformation (O1 to C7 distance = 6.691(2) Å) and it is stabilized in the wide rim of the cavity, hydrogen bonded with a secondary methoxy group of the host. As a result, *β*-citronellol is found significantly less disordered than *gr* in the TM-*β*-CD cavity, occupying only one site (100%) [23]. This is once more an evidence of the induce-fit mechanism, which is always more pronounced in the cases of the inclusion complexes with the flexible TM-*β*-CD as a host, affecting the conformation of

both host and guest. MD studies given below, show that the interconversions between different inclusion modes are significantly less for β-citronellol than *gr* in TM-β-CD (Fig. 8a). However, as in both cases (*gr*/TM-β-CD and β-citronellol/TM-β-CD) the main part of the guest protrudes from the wide rim of the host, the complex units are arranged similarly in the crystal packing. Even the hydration degree is the same in both crystal structures as in β-citronellol/TM-β-CD there was also found just a half occupied water site hydrogen bonded with an etheric O5 atom of the host.

3.4. Molecular dynamics studies

The crystallographically determined structures of *gr*/β-CD, *gr*/DM-β-CD and *gr*/TM-β-CD inclusion complexes (host:guest ratio 2:2, 1:1 and 1:1, respectively), excluding water molecules of hydration, were used as three distinct starting models. Prior to MD runs, the models were subjected to equilibration and the subsequent molecular dynamics simulations were carried out at 300 K in explicit water solvent for almost 12 ns as described in paragraph 2.3.

In the case of *gr*/β-CD, the starting model comprises of a duet of guests (*gr*1A and *gr*1B), encapsulated in a head-head β-CD dimer. By monitoring the frames during the time interval of the simulation, we observed that the guest molecules rotate about the seven fold molecular axis of the hosts retaining their initial orientation in a stable β-CD dimer. The hydroxyl groups of the guests are almost always hydrogen bonded with alternate primary hydroxyls of the hosts whereas their aliphatic ends, located in the interface of the dimer, form closed-shell weak H ···H interactions with the inner hydrogens (H3) of the secondary rim of the hosts. Both molecules fluctuate "up and down" inside the cavity varying their depth of immersion and consequently the height of their protrusion from the narrow rims of the dimer. The variation of the distance between O1 atom of the guests (*gr*1A and *gr*1B) and the O4 mean plane of their respective host (hostA and hostB) during the time interval of the simulation is shown in the Supplementary Fig. S1. This dynamic behavior resembles that of β-citronellol (*cl*) in the same host (Fig. 6a). Fig. 6b shows the distance between the O1 and C7 atoms of the guests for both *gr*/β-CD and *cl*/β-CD complexes. The variation of theses values for both terpenes indicates a preference for extended conformation inside the apolar environment of the dimeric β-CD cavity. In Fig. 6c, the value of the C4—C5—C6—C7 dihedral angle as a function of time in both complexes is also plotted. It may be clearly seen that this dihedral angle fluctuates around a value of −100° or +100° in both cases.

In the case of the *gr*/DM-β-CD inclusion complex, we observed that the guest molecule also remains encapsulated 'axially' inside the hydrophobic DM-β-CD cavity during the 12 ns simulation, rotating about the seven fold molecular axis of the host. As DM-β-CD retains its open cone conformation, the hydroxyl group of the guest projects always through the primary rim of the host forming hydrogen bonds with oxygens of alternate primary methoxy groups and water molecules. Its aliphatic end is located in the secondary rim of the host when its hydroxyl group is H-bonded with a host's primary methoxy group whereas it is deeply immersed in the hydrophobic cavity of the host when its hydroxyl forms H-bonds with solvent water molecules. The depth of immersion of the guest in the hydrophobic cavity of the host varies accordingly (Supplementary Fig. S2).

The MD simulation for the β-citronellol/DM-β-CD showed that the guest β-citronellol presents similar dynamic behavior to that of *gr* in DM-β-CD (Fig. 7a). However, some differences are observed in the variation of the conformation of these two guests. In particular, the distance between the O1 and C7 atom of the guest, shown in Fig. 7b, is most of the time larger for *gr* than β-citronellol, indicating a more extended conformation for *gr*. Moreover, the values of the C4—C5—C6—C7 dihedral angle as a function of time given in Fig. 7c for both inclusion complexes, fluctuate around −100° or +100° for β-citronellol whereas they are distributed mainly around 180° for *gr*. Thus, the rigid hydrophobic interior of DM-β-CD offers the space and the environment that allows β-citronellol to adopt more relaxed conformations whereas *gr*, unable to bend as the β-citronellol molecule, is found adopting more extended and rigid conformations.

In the case of *gr*/TM-β-CD, the guest is found most of the time accommodated 'equatorially' in the wide (secondary) rim of the host. TM-β-CD macrocycle, far deviating from a regular heptagon, is significantly distorted during the time frame of the simulation. Its primary rim remains 'closed' not allowing to the hydroxyl group of the guest to penetrate the primary methoxy groups 'lid'. Thus, the hydroxyl of the guest is located in the wide rim of the host, hydrogen bonded mainly with the secondary methoxy groups of the host (Fig. 8a). In the short time intervals where these H-bonds are not observed, the guest is accommodated axially but with opposite orientation to that of the guest in *gr*/β-CD and DM-β-CD inclusion complexes, i.e. with its aliphatic chain oriented towards the primary rim of the host and its hydroxyl group fully exposed to the polar solvent from the wide rim of the host. This inclusion mode is not stable, as the hydroxyl of the guest quickly reforms H-bonds with the methoxy groups of the host and the guest turns back to its initial equatorial position.

The MD simulation for the β-citronellol/TM-β-CD inclusion complex showed that the guest β-citronellol, being more flexible than *gr*, triggers better the induce-fit mechanism in its complexation with the also flexible TM-β-CD host. Fig. 8a shows clearly a lower RMSD for both host and guest molecules in the case of β-citronellol/TM-β-CD than *gr*/TM-β-CD. The plots of the distance between the O1 and C7 atom of the guests and the plots of the dihedral angle C4—C5—C6—C7 values over time for both *gr* and β-citronellol inclusion complexes with TM-β-CD (Fig. 8b) show that β-citronellol is found more relaxed than *gr* in the TM-β-CD cavity and it is not subtended to the abrupt conformational changes observed in the case of the *gr* guest.

In order to estimate the binding affinity in the case of the *gr*/β-CD inclusion complex, two separate calculations were made as follows: (i) calculation of the binding energy of the guest *gr*1 using the system of the two hosts (hostA and hostB) and the *gr*2 molecule as receptor and (ii) calculation of the binding energy of *gr*2 guest using the two hosts and the *gr*1 as receptor. Both calculations resulted in similar values indicating the formation of a stable inclusion complex mainly via van der Waals interactions (Supplementary Table S3). These values are very close to those calculated for the β-citronellol(*cl*)/β-CD indicating the formation of equally stable inclusion complexes in both cases (Table 2**)**.

In the case of the *gr*/DM-β-CD inclusion complex (1:1 guest:host stoichiometry), the calculated binding affinity is lower than that of *gr*/β-CD and of β-citronellol/DM-β-CD but still within the error margins of the method. Thus, *gr*/DM-β-CD can be also considered as a stable inclusion complex. On the other hand, the binding energy calculated for the *gr*/TM-β-CD is significant lower compared to that of *gr*/β-CD and lower but still within the error margins than that of *gr*/DM-β-CD confirming the inefficient inclusion of the guest in the hydrophobic cavity of the permethylated CD.

4. Conclusions

The *gr*/β-CD inclusion complex is found crystallized in a different form (Form II) than that previously reported by Ceborska et al. (Form I) [22] revealing a polymorphism for this inclusion complex. In both forms, two geraniol molecules are found

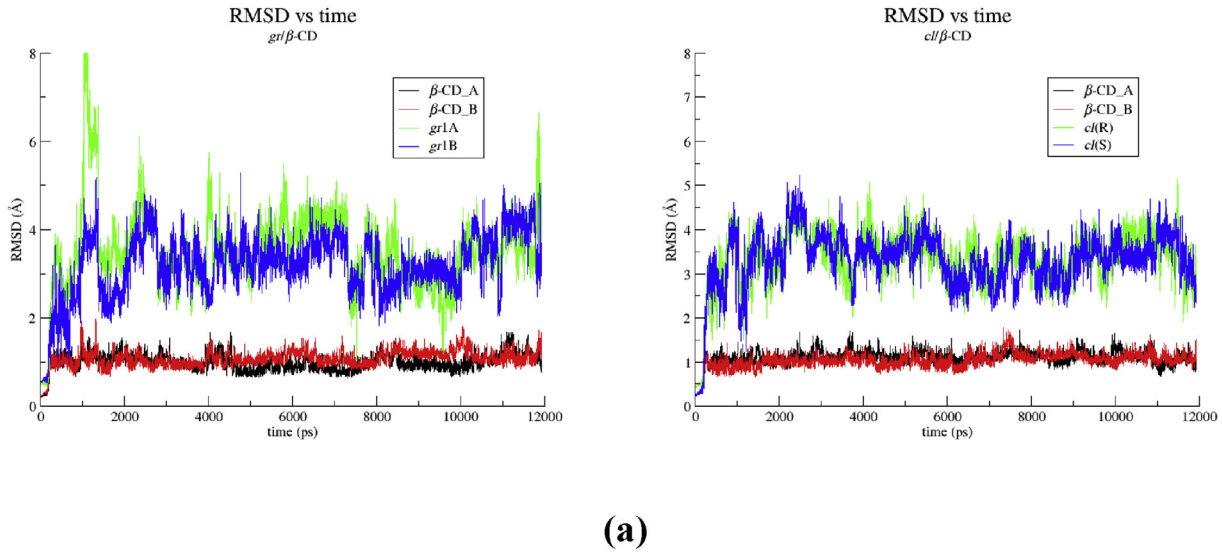

(a)

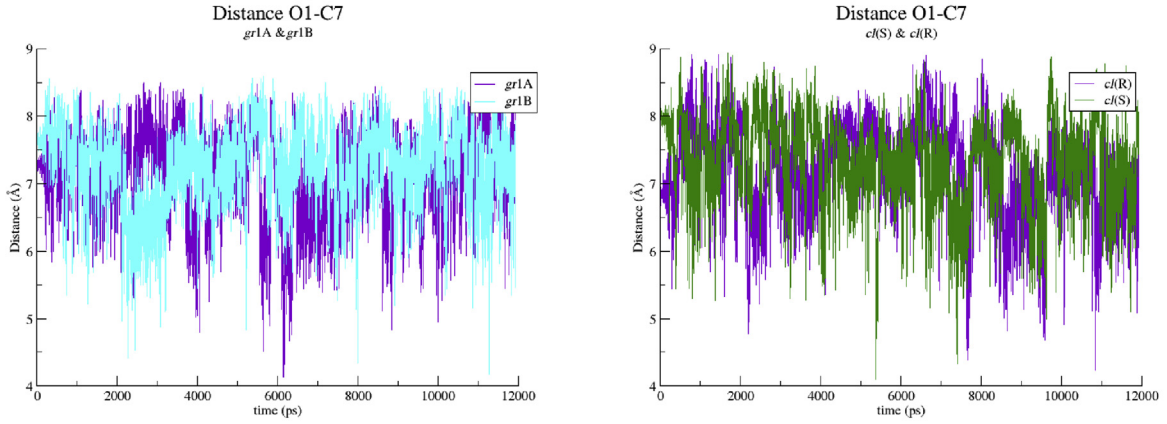

(b)

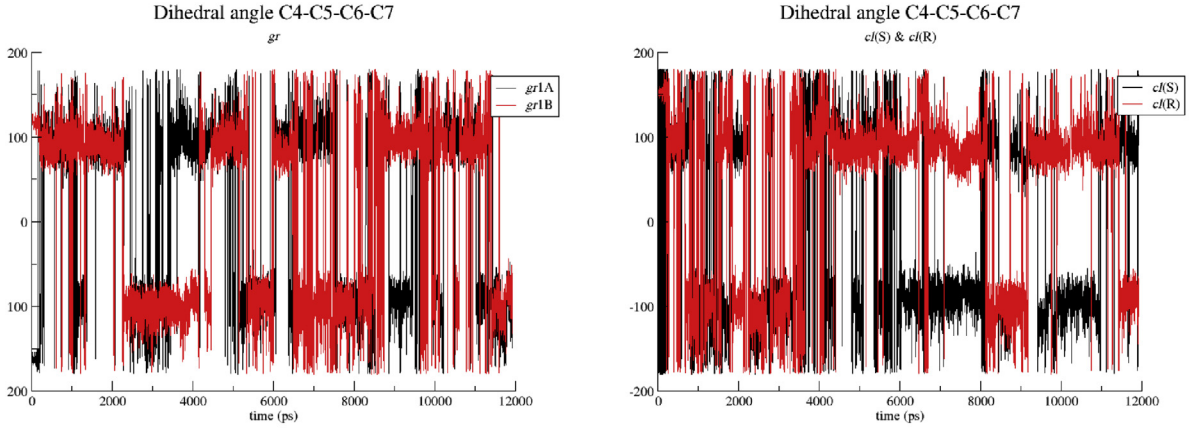

(c)

Fig. 6. **(a)** RMSD vs time for *gr*/*β*-CD and for *β*-citronellol (*cl*)/*β*-CD dimers (**b**) monitoring the distance between O1 and C7 atoms of geraniol and between O1 and C7 atoms of *β*-citronellol (*cl*) during the respective simulations and **(c)** plot of the dihedral angle C4—C5—C6—C7 vs time for the two geraniol and the two *β*-citronellol (*cl*) molecules inside the *β*-CD dimeric cavity.

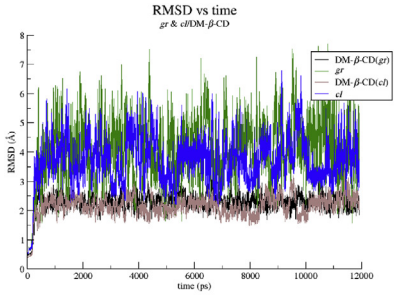

(a)

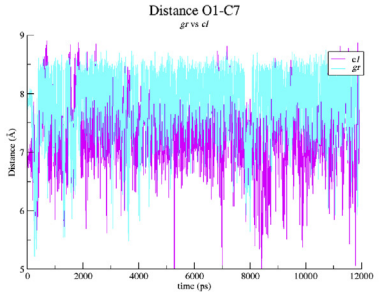

(b)

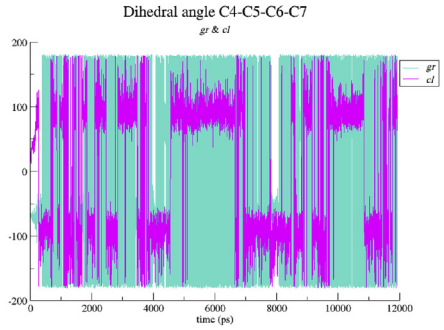

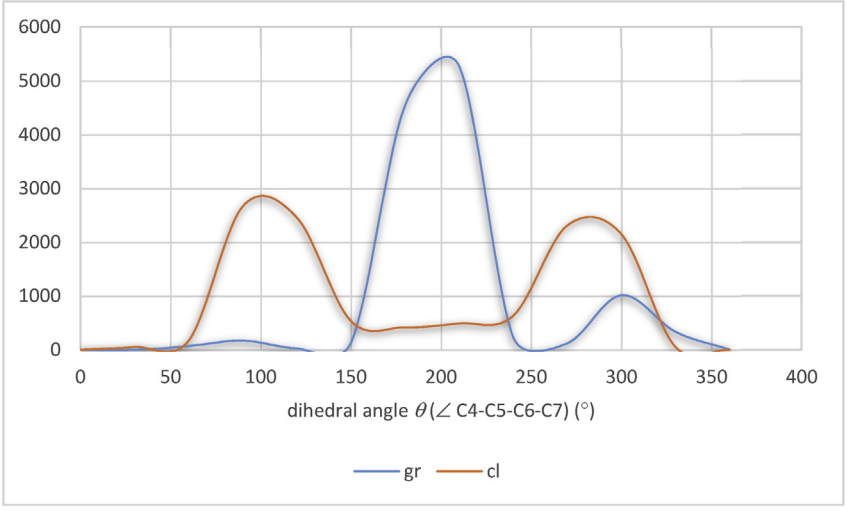

(c)

Fig. 7. **(a)** RMSD vs time for *gr*/DM-*β*-CD and *β*-citronellol(*cl*)/DM-*β*-CD inclusion complexes **(b)** plot of the distance between O1 and C7 atoms of geraniol (*gr*) and *β*-citronellol (*cl*) molecules inside the DM-*β*-CD cavity vs time and **(c)** plot of the dihedral angle C4–C5–C6–C7 vs time for geraniol (*gr*) and *β*-citronellol (*cl*) molecules inside the DM-*β*-CD cavity (left). The distribution of the dihedral angle *θ* (C4–C5–C6–C7) values for *gr* and *cl* inside the DM-*β*-CD cavity (right).

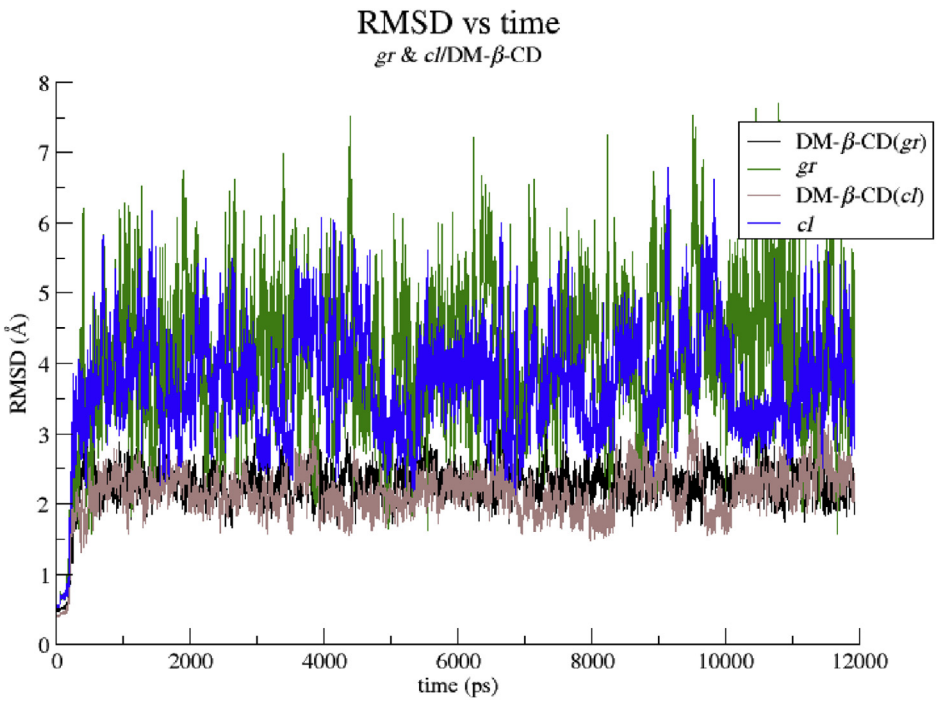

(a)

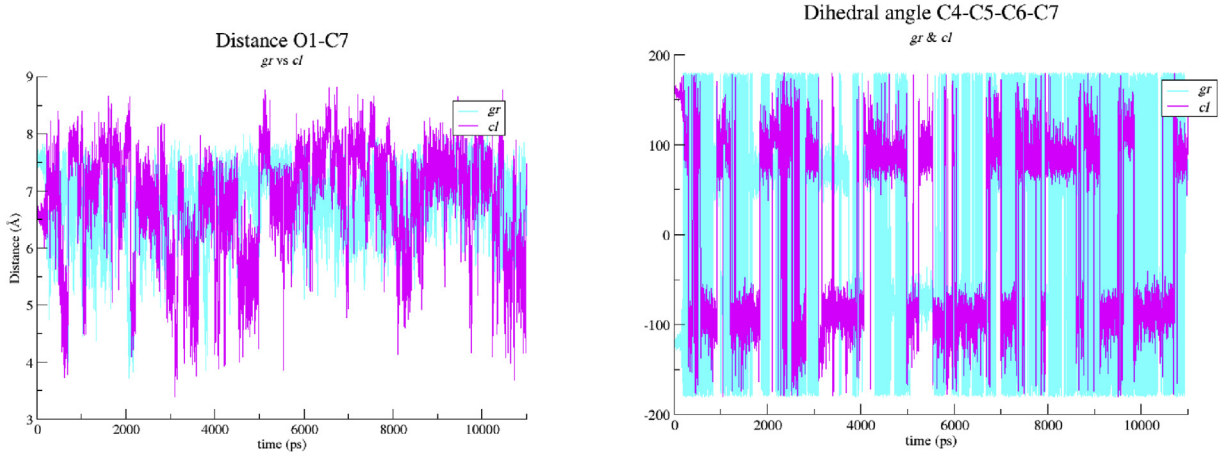

(b)

Fig. 8. **(a)** RMSD vs time for *gr*/TM-β-CD and for β-citronellol(*cl*)/TM-β-CD inclusion complex and (**b**) plots of the distance between the O1 and C7 atoms (left) and the dihedral angle C4−C5−C6−C7 (right) vs time for the *gr* and β-citronellol(*cl*) guests in TM-β-CD.

encapsulated in a head-to-head β-CD dimer adopting extended conformations. However, the form of the complex reported here (Form II) crystallizes in the $P2_1$ instead of the $P1$ space group of the Form I and the complex units are arranged according to the Channel (*CH*) packing mode along the *a*-axis instead of the Intermediate (*IM*) packing mode observed in Form I. The different crystal packing observed in these two forms is due to the different height of protrusion of the guests from the narrow rims of the dimeric host. This in turn is caused by the more or less extended conformation that the guest molecules adopt upon their complexation with the β-CDs in these two forms. In the crystal structure presented here (Form II), the encapsulated geraniol molecules adopt a less extended conformation that allows the dimeric complex units to form channels in which the guest molecules of adjacent dimers are

Table 2
The results from the MM/GBSA method for both geraniol (*gr*) and β-citronellol(*cl*) in their inclusion complex with native and two methylated β-CD. All units and their standard deviations are given in kcal/mol.

	Enthalpic term $\Delta G_{(GB)}$	STD	Entropic term $T\cdot\Delta S$	STD	Binding Energy ΔG_{all}	STD
gr1A/β-CD	−21.05	±2.08	−16.88	±2.41	−4.17	±3.19
gr1B/β-CD	−20.95	±2.02	−17.41	±2.30	−3.55	±3.06
gr/DM-β-CD	−18.65	±2.37	−16.01	±1.44	−2.64	±2.77
gr/TM-β-CD	−16.52	±2.88	−17.22	±2.00	0.70	±3.5
[a]*cl*(*R*)/β-CD	−21.21	±1.95	−17.51	±2.21	−3.71	±2.95
[a]*cl*(*S*)/β-CD	−21.94	±2.05	−17.26	±2.58	−4.68	±3.29
[a]*cl*/DM-β-CD	−20.14	±2.73	−16.54	±1.71	−3.59	±3.22
[a]*cl*/TM-β-CD	−12.46	±4.05	−16.02	±1.71	3.57	±4.40

gr: geraniol.
cl: β-citronellol.
[a] [23].

interconnected via CH ···O and hydrogen bonds forming an internal wire.

The *gr*/DM-β-CD inclusion complex crystallizes in the $P2_12_12_1$ space group. In the complex unit, the host DM-β-CD adopts the conformation of a rigid and well-shaped open cone in which the guest molecule is found highly disordered over 5 sites with varying depths of immersion. DM-β-CDs are arranged in a head-to-tail mode in channels hosting geraniol molecules that are interconnected via CH ···O bonds.

The *gr*/TM-β-CD inclusion complex also crystallizes in the $P2_12_12_1$ space group. In this case, the host being more flexible due to the absence of intramolecular interglucose hydrogen bonds, is found with a severely distorted macrocycle and a 'closed' cup-shaped conformation. The guest geraniol molecule cannot penetrate the 'lid' of the host and it is accommodated equatorially in the wide rim of the host with its main part laying outside of the host cavity in the intermediate space between the succeeding hosts. The guest is found disordered over 3 sites with quite different orientations.

The MD analysis based on the above crystal structures sheds light on the dynamic behavior of the geraniol upon inclusion complexation with these hosts, its conformation variations and the possible interconversions of the inclusion modes in solution. By comparing these results to those of the MD analysis of β-citronellol inclusion complexes with the same hosts the following conclusions are drawn: β-citronellol has the same dynamic behavior as geraniol upon complexation with β-CD where the guest molecules are similarly accommodated inside a rigid dimeric β-CD cavity. On the other hand, β-citronellol, having a degree of torsional freedom more and thus being more flexible than geraniol, can trigger better than geraniol the induce-fit mechanism in the complexation process with the rigid DM-β-CD and especially the flexible TM-β-CD host. In the cases of these complexes the guest β-citronellol is found much less disordered than geraniol. Finally, MM/GBSA-calculations performed for comparison of the inclusion complexes binding affinity with each other. The results revealed that the ascending order in ΔG values is: *gr*/TM-β-CD < *gr*/DM-β-CD < *gr*/β-CD. The same order was observed for the β-citronellol inclusion complexes with the same hosts [23].

Funding

We acknowledge support of this work by the project **"**GR-OPENSCREEN-Open Access Research Infrastructure for targeted technologies for scanning and bioactive molecules to protect Health, Livestock, Agriculture and the Environment" (Grant MIS 5002691).

Declaration of competing interest

The authors declare that the research was conducted in the absence of any commercial or financial relationships that could be construed as a potential conflict of interest.

Acknowledgements

We thank the European Community, Research Infrastructure Action under the FP6 "Structuring the European Research Area Specific Programme", Contract Number RII3-CT-2004-506008 for support of the work of data collection at the EMBL X11 beamline at the DORIS storage ring, DESY, Hamburg (Project no: PX-07-91). We also thank, Prof. Elias E. Eliopoulos for his useful comments and suggestions.

Appendix A. Supplementary data

Supplementary data to this article can be found online at https://doi.org/10.1016/j.molstruc.2019.127350.

References

[1] W. Chen, A.M. Viljoen, Geraniol — a review of a commercially important fragrance material, Chem. Divers. Biol. Funct. Plant Volatiles. 76 (2010) 643–651, https://doi.org/10.1016/j.sajb.2010.05.008.
[2] W. Dhifi, S. Bellili, S. Jazi, N. Bahloul, W. Mnif, Essential oils' chemical characterization and investigation of some biological activities: a critical review, Medicine 3 (2016) 25, https://doi.org/10.3390/medicines3040025.
[3] X. Tang, Y.-L. Shao, Y.-J. Tang, W.-W. Zhou, Antifungal activity of essential oil compounds (geraniol and citral) and inhibitory mechanisms on grain pathogens (*Aspergillus flavus* and *Aspergillus ochraceus*), Molecules 23 (2018), https://doi.org/10.3390/molecules23092108.
[4] L. Vasireddy, L.E.H. Bingle, M.S. Davies, Antimicrobial activity of essential oils against multidrug-resistant clinical isolates of the *Burkholderia cepacia* complex, PLoS One 13 (2018), e0201835, https://doi.org/10.1371/journal.pone.0201835.
[5] O. Kosakowska, K. Baczek, J.L. Przybyl, E. Pioro-Jabrucka, W. Czupa, A. Synowiec, M. Gniewosz, R. Costa, L. Mondello, Z. Weglarz, Antioxidant and antibacterial activity of roseroot (*Rhodiola rosea* L.) dry extracts, Molecules 23 (2018) 1767, https://doi.org/10.3390/molecules23071767.
[6] G.C. Müller, A. Junnila, J. Butler, V.D. Kravchenko, E.E. Revay, R.W. Weiss, Y. Schlein, Efficacy of the botanical repellents geraniol, linalool, and citronella against mosquitoes, J. Vector Ecol. 34 (2009) 2–8, https://doi.org/10.1111/j.1948-7134.2009.00002.x.
[7] S. Carnesecchi, Y. Schneider, J. Ceraline, B. Duranton, F. Gosse, N. Seiler, F. Raul, Geraniol, a component of plant essential oils, inhibits growth and polyamine biosynthesis in human colon cancer cells, J. Pharmacol. Exp. Ther. 298 (2001) 197–200.
[8] S. Carnesecchi, R. Bras-Goncalves, A. Bradaia, M. Zeisel, F. Gosse, M.-F. Poupon, F. Raul, Geraniol, a component of plant essential oils, modulates DNA synthesis and potentiates 5-fluorouracil efficacy on human colon tumor xenografts, Cancer Lett. 215 (2004) 53–59, https://doi.org/10.1016/j.canlet.2004.06.019.
[9] L. Hagvall, J.M. Baron, A. Börje, L. Weidolf, H. Merk, A.-T. Karlberg, Cytochrome P450-mediated activation of the fragrance compound geraniol forms potent contact allergens, Toxicol. Appl. Pharmacol. 233 (2008) 308–313, https://

doi.org/10.1016/j.taap.2008.08.014.
[10] A.C.C. Santos, P.F. Cristaldo, A.P.A. Araujo, C.R. Melo, A.P.S. Lima, E.D.R. Santana, B.M.S. de Oliveira, J.W.S. Oliveira, J.S. Vieira, A.F. Blank, L. Bacci, Apis mellifera (Insecta: hymenoptera) in the target of neonicotinoids: a one-way ticket? Bioinsecticides can be an alternative, Ecotoxicol. Environ. Saf. 163 (2018) 28–36, https://doi.org/10.1016/j.ecoenv.2018.07.048.
[11] A. Lapczynski, R.J. Foxenberg, S.P. Bhatia, C.S. Letizia, A.M. Api, Fragrance material review on nerol, Food Chem. Toxicol. Int. J. Publ. Br. Ind. Biol. Res. Assoc. 46 (Suppl 11) (2008) S241–S244, https://doi.org/10.1016/j.fct.2008.06.062.
[12] A. Lapczynski, C.S. Letizia, A.M. Api, Fragrance material review on (+)-(R)-citronellol, Food Chem. Toxicol. 46 (2008) S114–S116, https://doi.org/10.1016/j.fct.2008.06.018.
[13] A. Lapczynski, S.P. Bhatia, R.J. Foxenberg, C.S. Letizia, A.M. Api, Fragrance material review on geraniol, Food Chem. Toxicol. 46 (2008) S160–S170, https://doi.org/10.1016/j.fct.2008.06.048.
[14] Z. Hadian, M. Maleki, K. Abdi, F. Atyabi, A. Mohammadi, R. Khaksar, Preparation and characterization of nanoparticle beta-cyclodextrin:geraniol inclusion complexes, Iran, J. Pharm. Res. 17 (2018) 39–51, https://doi.org/10.22037/IJPR.2018.2153.
[15] F. Kayaci, H.S. Sen, E. Durgun, T. Uyar, Functional electrospun polymeric nanofibers incorporating geraniol–cyclodextrin inclusion complexes: high thermal stability and enhanced durability of geraniol, Food Res. Int. 62 (2014) 424–431, https://doi.org/10.1016/j.foodres.2014.03.033.
[16] G. Astray, C. Gonzalez-Barreiro, J.C. Mejuto, R. Rial-Otero, J. Simal-Gándara, A review on the use of cyclodextrins in foods, Food Hydrocolloids 23 (2009) 1631–1640, https://doi.org/10.1016/j.foodhyd.2009.01.001.
[17] E.M.M.D. Valle, Cyclodextrins and their uses: a review, Process Biochem. 39 (2004) 1033–1046, https://doi.org/10.1016/S0032-9592(03)00258-9.
[18] B. Gidwani, A. Vyas, A comprehensive review on cyclodextrin-based carriers for delivery of chemotherapeutic cytotoxic anticancer drugs, BioMed Res. Int. 2015 (2015), 198268, https://doi.org/10.1155/2015/198268.
[19] S.V. Kurkov, T. Loftsson, Cyclodextrins., Int. J. Pharm. 453 (2013) 167–180, https://doi.org/10.1016/j.ijpharm.2012.06.055.
[20] M.D. López, M.J. Pascual-Villalobos, Analysis of monoterpenoids in inclusion complexes with β-cyclodextrin and study on ratio effect in these microcapsules, in: Proceedings of the 10th International Working Conference on Stored Product Protection, Julius-Kühn-Archiv, 2010, p. 425, https://doi.org/10.5073/jka.2010.425.220.
[21] I. Mourtzinos, N. Kalogeropoulos, S.E. Papadakis, K. Konstantinou, V.T. Karathanos, Encapsulation of nutraceutical monoterpenes in beta-cyclodextrin and modified starch, J. Food Sci. 73 (2008) S89–S94, https://doi.org/10.1111/j.1750-3841.2007.00609.x.
[22] M. Ceborska, K. Szwed, M. Asztemborska, M. Wszelaka-Rylik, E. Kicińska, K. Suwińska, Study of β-cyclodextrin inclusion complexes with volatile molecules geraniol and α-terpineol enantiomers in solid state and in solution, Chem. Phys. Lett. 641 (2015) 44–50, https://doi.org/10.1016/j.cplett.2015.10.018.
[23] K. Fourtaka, E. Christoforides, D. Mentzafos, K. Bethanis, Crystal structures and molecular dynamics studies of the inclusion compounds of β-citronellol in β-cyclodextrin, heptakis(2,6-di-O-methyl)-β-cyclodextrin and heptakis(2,3,6-tri-O-methyl)-β-cyclodextrin, J. Mol. Struct. 1161 (2018) 1–8, https://doi.org/10.1016/j.molstruc.2018.02.037.
[24] M.F. Maia, S.J. Moore, Plant-based insect repellents: a review of their efficacy, development and testing, Malar. J. 10 (2011), https://doi.org/10.1186/1475-2875-10-S1-S11. S11–S11.
[25] J.L. de Oliveira, E.V.R. Campos, A.E.S. Pereira, L.E.S. Nunes, C.C.L. da Silva, T. Pasquoto, R. Lima, G. Smaniotto, R.A. Polanczyk, L.F. Fraceto, Geraniol encapsulated in chitosan/gum Arabic nanoparticles: a promising system for pest management in sustainable agriculture, J. Agric. Food Chem. 66 (2018) 5325–5334, https://doi.org/10.1021/acs.jafc.8b00331.
[26] W. Kabsch, XDS, Acta Crystallogr. D Biol. Crystallogr. 66 (2010) 125–132, https://doi.org/10.1107/S0907444909047337.
[27] G.M. Sheldrick, SADABS Version 2012/1, 1, Bruker-AXS, Madison, Wisconsin, USA (2012).
[28] G.M. Sheldrick, XDS2SAD, University of Gottingen, Germany (2008).
[29] P.T. Beurskens, G. Beurskens, R. de Gelder, S. Garcia-Granda, R.O. Gould, J.M.M. Smits, The DIRDIF2008 Program System, Crystallography Laboratory, University of Nijmegen, The Netherlands.
[30] F. Tsorteki, K. Bethanis, D. Mentzafos, Structure of the inclusion complexes of heptakis(2,3,6-tri-O-methyl)-beta-cyclodextrin with indole-3-butyric acid and 2,4-dichlorophenoxyacetic acid, Carbohydr. Res. 339 (2004) 233–240.
[31] SAINT, Bruker-AXS, Version 8.34A, Madison, Wisconsin, USA, 2013.
[32] G.M. Sheldrick, Experimental phasing with *SHELXC/D/E*: combining chain tracing with density modification, Acta Crystallogr. D 66 (2010) 479–485, https://doi.org/10.1107/S0907444909038360.
[33] G.M. Sheldrick, Crystal structure refinement with *SHELXL*, Acta Crystallogr. C 71 (2015) 3–8, https://doi.org/10.1107/S2053229614024218.
[34] L.J. Farrugia, *WinGX* and *ORTEP* for windows: an update, J. Appl. Crystallogr. 45 (2012) 849–854, https://doi.org/10.1107/S0021889812029111.
[35] C.B. Hübschle, G.M. Sheldrick, B. Dittrich, *ShelXle*: a Qt graphical user interface for *SHELXL*, J. Appl. Crystallogr. 44 (2011) 1281–1284, https://doi.org/10.1107/S0021889811043202.
[36] A.W. Schüttelkopf, D.M.F. van Aalten, *PRODRG*: a tool for high-throughput crystallography of protein–ligand complexes, Acta Crystallogr. D Biol. Crystallogr. 60 (2004) 1355–1363, https://doi.org/10.1107/S0907444904011679.
[37] C.F. Macrae, I.J. Bruno, J.A. Chisholm, P.R. Edgington, P. McCabe, E. Pidcock, L. Rodriguez-Monge, R. Taylor, J. van de Streek, P.A. Wood, *Mercury CSD* 2.0 – new features for the visualization and investigation of crystal structures, J. Appl. Crystallogr. 41 (2008) 466–470, https://doi.org/10.1107/S0021889807067908.
[38] W.L. DeLano, The PyMOL Molecular Graphics System, DeLano Scientific LLC, San Carlos, CA, 2002.
[39] O.V. Dolomanov, L.J. Bourhis, R.J. Gildea, J.A.K. Howard, H. Puschmann, *OLEX2*: a complete structure solution, refinement and analysis program, J. Appl. Crystallogr. 42 (2009) 339–341, https://doi.org/10.1107/S0021889808042726.
[40] D.A. Case, T.E. Cheatham, T. Darden, H. Gohlke, R. Luo, K.M. Merz, A. Onufriev, C. Simmerling, B. Wang, R.J. Woods, The Amber biomolecular simulation programs, J. Comput. Chem. 26 (2005) 1668–1688, https://doi.org/10.1002/jcc.20290.
[41] K.N. Kirschner, A.B. Yongye, S.M. Tschampel, J. González-Outeiriño, C.R. Daniels, B.L. Foley, R.J. Woods, GLYCAM06: a generalizable biomolecular force field, Carbohydrates, J. Comput. Chem. 29 (2008) 622–655, https://doi.org/10.1002/jcc.20820.
[42] C. Cezard, X. Trivelli, F. Aubry, F. Djedaini-Pilard, F.-Y. Dupradeau, Molecular dynamics studies of native and substituted cyclodextrins in different media: 1. Charge derivation and force field performances, Phys. Chem. Chem. Phys. 13 (2011) 15103–15121, https://doi.org/10.1039/C1CP20854C.
[43] J. Wang, W. Wang, P.A. Kollman, D.A. Case, Automatic atom type and bond type perception in molecular mechanical calculations, J. Mol. Graph. Model. 25 (2006) 247–260, https://doi.org/10.1016/j.jmgm.2005.12.005.
[44] E. Christoforides, K. Bethanis, Chapter 3. Molecular dynamics studies of cyclodextrin inclusion compounds, in: Mark S. Kemp (Ed.), Book: an Introduction to Molecular Dynamics, Publisher: Nova Science Publishers, Inc, Suite N Hauppauge, NY, 11788 USA, 2019, pp. 109–142, 978-1-53616-054-3,415 Oser Avenue, https://novapublishers.com/shop/an-introduction-to-molecular-dynamics/.
[45] D.R. Roe, T.E. Cheatham 3rd, PTRAJ and CPPTRAJ: software for processing and analysis of molecular dynamics trajectory data, J. Chem. Theory Comput. 9 (2013) 3084–3095, https://doi.org/10.1021/ct400341p.
[46] W. Humphrey, A. Dalke, K. Schulten, VMD: visual molecular dynamics, J. Mol. Graph. 14 (1996) 33–38, https://doi.org/10.1016/0263-7855(96)00018-5.
[47] B.R. Miller 3rd, T.D.J. McGee, J.M. Swails, N. Homeyer, H. Gohlke, A.E. Roitberg, MMPBSA.py: an efficient program for end-state free energy calculations, J. Chem. Theory Comput. 8 (2012) 3314–3321, https://doi.org/10.1021/ct300418h.
[48] S. Genheden, U. Ryde, The MM/PBSA and MM/GBSA methods to estimate ligand-binding affinities, Expert Opin. Drug Discov. 10 (2015) 449–461, https://doi.org/10.1517/17460441.2015.1032936.
[49] D. Mentzafos, I.M. Mavridis, G. Le Bas, G. Tsoucaris, Structure of the 4-*tert*-butylbenzyl alcohol–β-cyclodextrin complex. Common features in the geometry of β-cyclodextrin dimeric complexes, Acta Crystallogr. B 47 (1991) 746–757, https://doi.org/10.1107/S010876819100366X.
[50] C.R. Groom, I.J. Bruno, M.P. Lightfoot, S.C. Ward, The Cambridge structural Database, Acta Crystallogr. B72 (2016) 171–179, https://doi.org/10.1107/S2052520616003954.
[51] K. Bethanis, E. Christoforides, F. Tsorteki, K. Fourtaka, D. Mentzafos, Structural studies of the inclusion compounds of α-naphthaleneacetic acid in heptakis(2,6-di-O-methyl)-β-Cyclodextrin and heptakis(2,3,6-tri-O-methyl)-β-Cyclodextrin by X-ray crystallography and molecular dynamics, J. Incl. Phenom. Macrocycl. Chem. 92 (2018) 157–171, https://doi.org/10.1007/s10847-018-0824-y.
[52] D.L. Cruickshank, N.M. Rougier, V.J. Maurel, R.H. de Rossi, E.I. Buján, S.A. Bourne, M.R. Caira, Permethylated β-cyclodextrin/pesticide complexes: X-ray structures and thermogravimetric assessment of kinetic parameters for complex dissociation, J. Incl. Phenom. Macrocycl. Chem. 75 (2013) 47–56, https://doi.org/10.1007/s10847-012-0145-5.
[53] D.L. Cruickshank, N.M. Rougier, V.J. Maurel, R.H. de Rossi, E.I. Buján, S.A. Bourne, M.R. Caira, Permethylated β-cyclodextrin/pesticide complexes: X-ray structures and thermogravimetric assessment of kinetic parameters for complex dissociation, J. Incl. Phenom. Macrocycl. Chem. 75 (2013) 47–56, https://doi.org/10.1007/s10847-012-0145-5.